IEEE Photonics Journal
An IEEE Photonics Society Publication

Open Access

# Transferred Flexible Three-Color Silicon Membrane Photodetector Arrays

Volume 7, Number 1, February 2015

**Laxmy Menon**
**Hongjun Yang, Member, IEEE**
**Sang June Cho**
**Solomon Mikael**
**Zhenqiang Ma, Senior Member, IEEE**
**Weidong Zhou, Senior Member, IEEE**

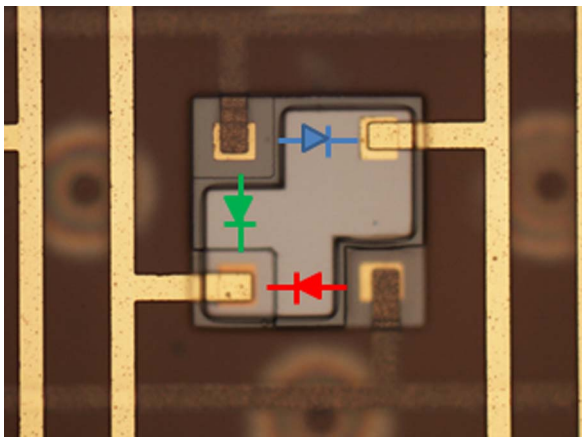

DOI: 10.1109/JPHOT.2014.2381660
1943-0655 

IEEE photonics SOCIETY

IEEE

# Transferred Flexible Three-Color Silicon Membrane Photodetector Arrays

**Laxmy Menon,[1] Hongjun Yang,[1,3] *Member, IEEE*, Sang June Cho,[2] Solomon Mikael,[2] Zhenqiang Ma,[2] *Senior Member, IEEE*, and Weidong Zhou,[1] *Senior Member, IEEE***

[1]Department of Electrical Engineering, University of Texas at Arlington, Arlington, TX 76019 USA
[2]Department of Electrical and Computer Engineering, University of Wisconsin-Madison, Madison, WI 53706 USA
[3]Semerane, Inc., Arlington, TX 76010 USA

*DOI: 10.1109/JPHOT.2014.2381660*


Manuscript received October 27, 2014; revised November 25, 2014; accepted December 2, 2014. Date of publication December 18, 2014; date of current version December 24, 2014. Corresponding author: W. Zhou (e-mail: wzhou@uta.edu).

**Abstract:** We report the design and fabrication of transfer-printed flexible three-color multijunction 8 × 8 crystalline silicon membrane photodetector arrays. Based on the penetration-depth-dependent absorption of different wavelengths, filter-free color detection can be obtained via three junction photocurrent measurement. The optical measurements show good agreements with the optical behavior predicted by the design and simulation. No noticeable changes were observed in the device performance when it was operated in a bending state.

**Index Terms:** Flexible electronics, focal plane arrays, photodetectors.

## 1. Introduction

Silicon multi-color photodetector (PD) arrays, capable of simultaneous sensing of light of multiple wavelengths by one pixel, are highly desirable for sensing and imaging applications. Common approaches in place today involve color discrimination based on optical filters with relatively slow refresh rate or compromised spatial resolutions. There have been several efforts made to stray away from the commonly used optical sensing with Color Filter Arrays (CFA), as they suffer from color aliasing effects (color moiré effect). Since three color filters are spatially arranged to form one color pixel, their resolution is limited. Several structures like PINIP, NIPIN, PININIP, NIPIIN, TCO/PINIP/TCO/PIN, PIIIN, PIN, and NIN have been explored to obtain two and three color detection with different materials, biasing, configurations and illumination conditions [1]–[6]. Vertically integrated structure, where the absorption of photons occur at different depths, depending on the wavelength of the incident light, can avoid the inevitable transmission loss, color aliasing effect and resolution limitation encountered with color filter array(CFA) based sensor arrays [7], [8].

Here we present a crystalline silicon membrane based flexible multi-color photodetector array, with a vertical n-p-n-p structure, capable of detecting blue, green and red colors of the visible spectrum by utilizing the wavelength dependent absorption property of silicon [9]. The thickness of each layer of the vertical structure has been optimized to match the absorption depth of blue, green and red wavelengths. The short wavelength light is absorbed near the surface of the

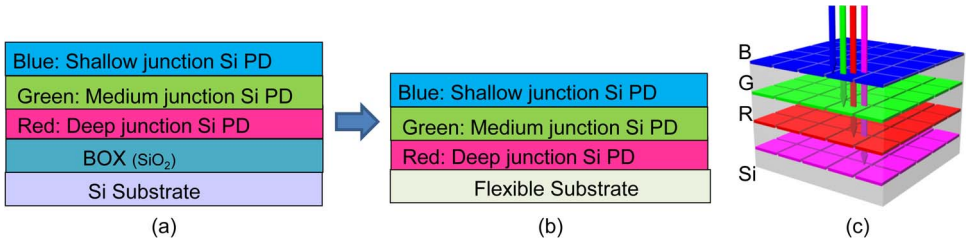


Fig. 1. Schematics of the proposed crystalline nanomembrane based stacked multi-color multi-band photodetector arrays: (a) Triple-junction Si PDs on SOI for red (R), green (G), and blue (B) color detection. (b) Flexible RGB color PDs based on transfer printed Si-PDs on flexible substrates. (c) Multi-color multi-band PDs based on transfer printed Si/InGaAs nanomembranes.

TABLE 1

Structure of SOI used for simulation and fabrication

| Material | Thickness | Doping | Concentration |
|---|---|---|---|
| Si | 0.2 μm | n+ | 1e18 |
| Si | 0.4 μm | p+ | 1e18 |
| Si | 1.4 μm | n+ | 1e18 |
| Si | 4.5 μm | p+ | 1e18 |
| $SiO_2$ (1.0 μm) | | | |
| Si-substrate (660 μm) | | | |

device, at the topmost junction and the long wavelength light is absorbed at larger depths, at the deepest junction. By appropriately biasing each p–n junction in the vertical structure, current can be extracted from the junctions, which will in turn provide the corresponding color information. Based on transfer printing process, these crystalline silicon membrane based photodetector arrays are transferred onto flexible kapton substrate, enabling high performance flexible photodetector arrays for potentially flexible focal plane array imaging and sensing applications.

## 2. Device Design

Based on the transfer printing process, we proposed and demonstrated multi-color multi-band flexible photodetector arrays based on crystalline silicon membranes and/or compound semiconductor membranes [10], [11]. Shown in Fig. 1 are the schematics of the proposed crystalline nanomembrane based stacked multi-color multi-band photodetector arrays. Starting with a design of triple-junction Si PDs on SOI for red (R), green (G), and blue (B) color detection [Fig. 1(a)], the structure can be released and transfer printed onto a foreign substrates [Fig. 1(b)], or stacked with other semiconductor materials for multi-band detection [Fig. 1(c)]. Notice the principle and process reported here can also be applied to a wide range of material systems, for multi-color multi-band imaging systems and spectrally resolved sensing systems. Thickness of each layer of the structure was optimized based on the penetration depth of blue, green and red wavelengths, and the design simulation was done using Taurus Medici software. Finally, the optimized structure is chosen with parameters shown in Table 1. Simulated responsivities for this design is also shown in Fig. 2 for the triple junction design. The structure was grown by IQE, Inc. Notice that peak responsivities for three junctions occur at three distinctive wavelengths (colors) with similar peak values of 0.1–0.16 A/W. Such design can enable optimal imaging sensitivity for three colors and high contrast color reconstruction based on imaging fusion techniques.

## 3. Device Fabrication

The process flow for the device fabrication is illustrated in Fig. 3. SOI substrate [Fig. 3(a)] is first patterned with release holes, and then etched to expose the underlying 1 $\mu$m thick buried oxide [BOX, Fig. 3(b)]. HF etching was done to remove this oxide and release the 6.5 $\mu$m thick Si

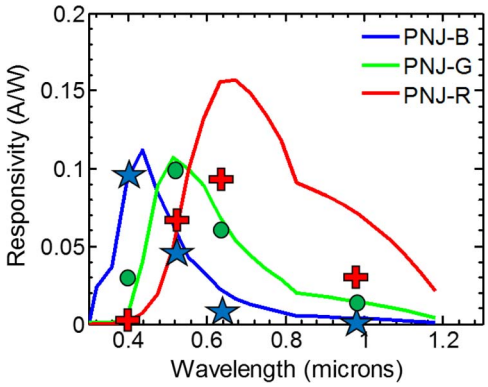


Fig. 2. Simulated (line) and measured (symbol) responsivities for the triple-junction RGB detector arrays. Tests were done with lasers at wavelengths of 405 nm, 532 nm, 630 nm, and 980 nm.

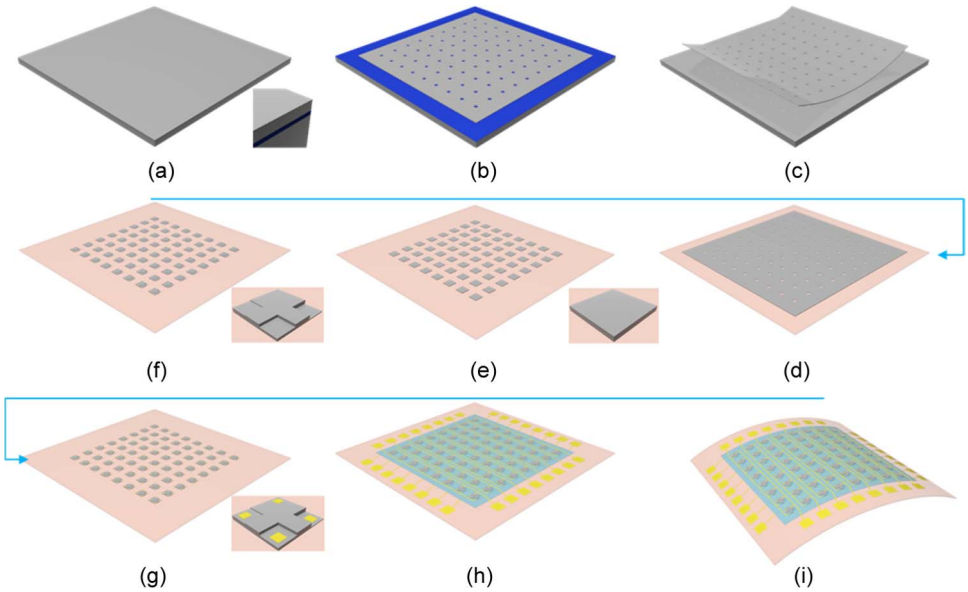


Fig. 3. Fabrication process flow: (a) SOI substrate; (b) etching release holes to remove box layer; (c) Si nanomembrane suspended after box etching; (d) Si nanomembrane transferred on Kapton with SU-8 as the adhesive layer; (e) etching individual pixels to form detector arrays; (f) etching the contact regions to access individual doped layers with different etching depths; (g) metallization of local contacts (inset) to individual doped layers on each pixel; (h) four Interconnect layers formed on two separate planes, with isolation provided by two polyimide passivation layers in between; and (i) completed flexible photodetector array on Kapton substrate.

nanomembrane as shown in Fig. 3(c). By wet transfer, this nanomembrane was transferred on to a SU-8 coated 125 $\mu$m thick Kapton sheet [Fig. 3(d)]. The transferred nanomembrane is 4.2 mm long, 4.3 mm wide, and the regular lithography process were then performed on the transferred Si nanomembrane on Kapton. The pixel mesa arrays were patterned with reactive ion etching (RIE) process to form mesa sizes of 100 $\mu$m $\times$ 100 $\mu$m [insert of Fig. 3(e)]; and the contact regions in each pixels were also defined by dry etching, followed by metallization of the local contacts at each depth [zoom-in view insert of Fig. 3(g)]. Four interconnect layers were subsequently formed with Cr/Au in two groups for the access of individual contacts of the Si-PD pixels in the PD array as shown in Fig. 3(h). It is worth to note here that HD4104 polyimide passivation layer was introduced for the isolation of individual interconnect lines at different depths. Shown in Fig. 3(i) is the final structure under bending.

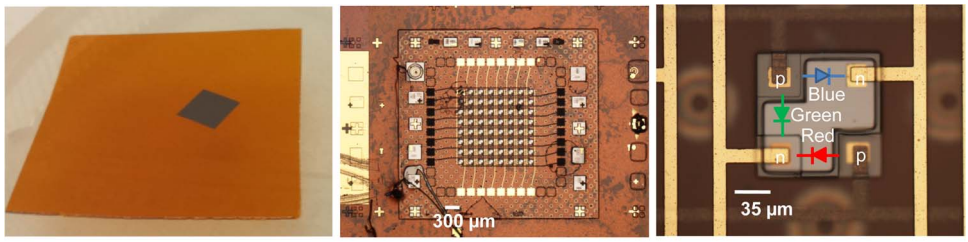


Fig. 4. Micrographs of (a) transferred crystalline Si membranes, and (b), (c) fabricated flexible 3-color Si membrane PD arrays.

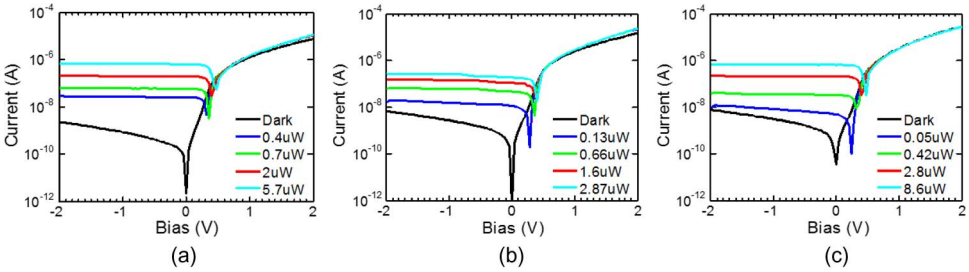


Fig. 5. Measured I–V characteristics of blue, green, and red junctions, under three incident wavelengths of (a) 405 nm, (b) 532 nm, and (c) 632 nm, respectively.

Micrographs of the fabricated devices on a kapton substrate are shown in Fig. 4. Shown in Fig. 4(a) is a transferred crystalline Si membrane on a kapton substrate before further device processing. Shown in Fig. 4(b) is a micrograph of 8 $\times$ 8 three color (four interconnect pad groups on four sides) photodetectors fabricated on the kapton substrate. As shown in Fig. 4(c), each pixel have four interconnect lines (on two layers) to provide individual access to each junctions on every pixel in the array.

## 4. Device Characterization

Individual pixels were first characterized, with typical results shown in Fig. 5, for the first (blue), second (green), and third (red) junctions measured under 405 nm, 532 nm, and 632 nm incident wavelength respectively. I–V measurements were done at room temperature using a Keithley 2612 current source. The dark currents for all junctions and devices tested show less than 10 nA over reverse bias voltage up to $-2$ V. For the illumination measurements, light was centered on the individual devices with a lensed fiber via a light wave probe system. Light response for each wavelength was done for various intensities and they showed a minimum of at least 2 orders of magnitude increase from the dark current. The measured responsivities for blue, green and red wavelengths are 0.1 A/W, 0.09 A/W, and 0.07 A/W, respectively. Additionally, each junction was also tested with two other wavelengths, to calibrate the color selective responstivities. All the results are shown in Fig. 2, with different symbols. Note excellent agreements were obtained for both blue (PN-J1) and green (PN-J2) junctions. Some discrepancies were found between measured and simulated responsitivities for red (PN-J3) junction, which may be related to the differences in the actual power being absorbed for this junction.

Array performance was also evaluated by measuring uniformity of pixel devices and the imaging capabilities. By measuring the spectral responsivities for each junction, color (spectral) information can be resolved based on post-imaging data process, which can be used to construct color images. Imaging was done using a QTH white light source that was focused on the 8 $\times$ 8 silicon photodetector array through a chrome mask with the letter “H”. On the array, the pixels that are not covered by the area of the letter “H” is illuminated by the light source. The resulting image formed after data handling is shown in Fig. 6. The horizontal and vertical numbers in the

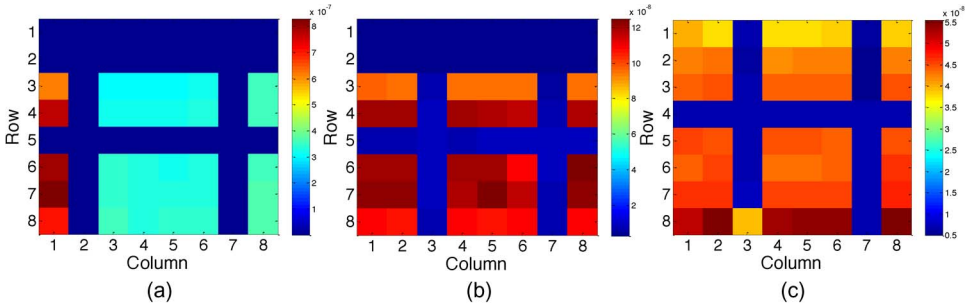


Fig. 6. Reproduced images of the letter "H" formed by biasing (a) blue junction, (b) green junction, and (c) red junction.

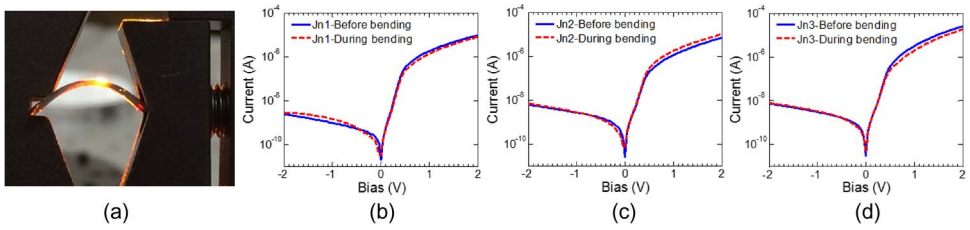


Fig. 7. Bending characteristics. (a) Device being tested on a bending stage. (b), (c), (d) Measured dark currents before and during bending for the junctions of blue, green, and red, respectively.

figure correspond to the row and column number of the array. The two horizontal blue rows in Fig. 6(a) and (b) occur due to lower responses in rows 1 and 2, as opposed to the others. Each square in the figures represent the difference in the measured response current and dark current for that specific pixel/device. The scale bar on the right side of each figure, shows the range of values in the square. Non-uniformity in this difference is depicted as difference in the color of pixels in the "non-H" region. Imaging quality can be improved by increasing the pixel size and improving the uniformity of the imager arrays. It is also worth noting that the illumination white light source used in our measurements is not ideally a collimated beam, which creates unnecessary shadow effect when the "H" chrome shadow mask is used for the imaging demonstration.

To demonstrate the flexibility of the photodetector array, bending tests were also performed. The kapton sheet housing the array was placed inside a lens/filter holder (with bending radius of 8 mm [12]) and the screws of the apparatus was adjusted to bend the kapton and hence the photodetector array. I–V measurements were taken while the device was in the bent state. A comparison of the dark currents before and during the bending (Fig. 7) shows that the device performance is maintained during the bending, and there is no noticeable degradation in dark current.

## 5. Conclusion

In conclusion, we have designed, fabricated, and characterized transfer printed flexible three-color multi-junction crystalline silicon membrane photodetector array. Since the device is a vertical structure which utilizes the depth dependent wavelength absorption property of silicon, the filters that are normally used in multicolor detectors can be avoided. Each of the 64 devices in the $8 \times 8$ array can be individually addressed and color information can be obtained from each detector in the array. We have obtained responsivities of 0.1 A/W, 0.09 A/W, and 0.07 A/W for blue, green and red colors respectively. This method can be extended to obtain higher pixel density for better image resolution. Bending tests performed on the device, show good performance during bending, which makes the photodetector array a good candidate for applications requiring flexibility.

## References


[1] J. Dresner, "Amorphous silicon p-i-n-i-p and n-i-p-i-n diodes," *Appl. Phys., Lett.*, vol. 48, no. 15, pp. 1006–1008, Apr. 1986.

[2] G. De Cesare, F. Irrera, F. Lemmi, and F. Palma, "Amorphous Si/SiC three-color detector with adjustable threshold," *Appl. Phys. Lett.*, vol. 66, no. 10, pp. 1178–1180, Mar. 1995.

[3] D. Knipp, H. Stiebig, J. Fölsch, F. Finger, and H. Wagner, "Amorphous silicon based nipiin structure for color detection," *J. Appl. Phys.*, vol. 83, no. 3, pp. 1463–1468, 1998.

[4] M. Topic, H. Stiebig, D. Knipp, and F. Smole, "Optimization of a-Si: H-based three-terminal three-color detectors," *IEEE Trans. Electron Devices*, vol. 46, no. 9, pp. 1839–1845, Sep. 1999.

[5] J. Zimmer, D. Knipp, H. Stiebig, and H. Wagner, "Amorphous silicon-based unipolar detector for color recognition," *IEEE Trans. Electron Devices*, vol. 46, no. 5, pp. 884–891, May 1999.

[6] H. Lee *et al.*, "Transient photoconductive gain in a-Si: H devices and its applications in radiation detection," *Nucl. Instrum. Methods Phys. Res., Sect. A: Accelerators, Spectrometers, Detectors Associated Equip.*, vol. 399, no. 2/3, pp. 324–334, Nov. 1997.

[7] R. F. Lyon and P. M. Hubel, "Eyeing the camera: Into the next century," in *Proc. Color Imag. Conf.*, 2002, pp. 349–355.

[8] D. Knipp, H. Stiebig, J. Fölsch, and H. Wagner, "Four terminal color detector for digital signal processing," *J. Non-Cryst. Solids*, vol. 227, pp. 1321–1325, May 1998.

[9] L. Menon, H. Yang, S. Wang, Z. Ma, and W. Zhou, "Flexible three-color silicon membrane photodetector arrays," presented at the *IEEE Photon. Conf.*, La Jolla, CA, USA, 2014.

[10] M. A. Meitl *et al.*, "Transfer printing by kinetic control of adhesion to an elastomeric stamp," *Nat. Mater.*, vol. 5, no. 1, pp. 33–38, 2005.

[11] W. Zhou *et al.*, "Progress in 2D photonic crystal Fano resonance photonics," *Prog. Quant. Electron.*, vol. 38, no. 1, pp. 1–74, Jan. 2014.

[12] S. I. Park *et al.*, "Theoretical and experimental studies of bending of inorganic electronic materials on plastic substrates," *Adv. Funct. Mater.*, vol. 18, no. 18, pp. 2673–2684, Sep. 2008.